Long pulse, high energy output at 365 nm from an frequency-doubled Alexandrite laser

Pan Qing*, Xiaoping Yang

Division of Manufacturing Science and Technology, CSIRO, Private Bag 33, Rosebank MDC, Clayton, Vic. 3169, Australia

Abstract

A high energy long pulse and low peak power at 365 nm ultra-violet laser is described. The laser at this wavelength is produced by the second harmonic generation of a flash-lamp pumped solid state Alexandrite laser. At optimum temperature, coherent 365 nm light of 186 mJ/pulse with 220 μs width is obtained without Q-switching. © 2001 Elsevier Science B.V. All rights reserved.

Keywords: Alexandrite; Lang pulse; Ultra-violet laser; Four-lever laser; Second harmonic generation; Walk-off

1. Introduction

Ultra-violet (UV) emission at 365 nm is one of the wavelength that can be used in the micro-electronics industries for optical lithography applications such as optical steppers to produce micron or sub-micron features on a wafer [1]. Traditionally UV light is generated from the I-line emission of a Mercury arc lamp, which requires a narrow filter of several nm bandwidth. This method can only produce light with limited energy and the light is not coherent, which limits optical lithography resolution and productivity. In addition, demands for higher resolution and larger depth of focus in microelectronic industries have required a shift in light source wavelength from 436 nm (Hg G-line) to the deep-UV (DUV). However, the traditional mercury arc lamp cannot produce sufficient energy in this region and an UV laser is essential. The excimer laser has been successfully in industrial applications where DUV (at 248 nm, using KrF) for resist exposure and a DUV stepper has recently been installed in the computer dynamic random acquire memory (DRAM) chips production line.

While the KrF laser at 248 nm has reached maturity for industrial applications, it suffers from some fundamental weaknesses. Like other gas lasers, the excimer laser is complex and it is expensive both to buy and to maintain. Solid state lasers, as opposed to gas lasers, provide reliability and are simple and easy to maintain. Solid state lasers also have high quantum efficiency, a long coherent length and a much better mode. Thus there is

---

* Corresponding author. Address: Opto-Electronics Institute, Shanxi University, Taiyuan, Shanxi, China. Tel.: +61-3-95452930; fax: +61-3-95452933/+86-351-701-1500.

E-mail address: panqing@sxu.edu.cn (P. Qing).

strong motivation to move from a gas laser to a solid state laser. In some cases however development of a solid state laser to replace a gas laser is limited by availability of the wavelengths from solid laser crystals, which are not as rich in fluorescent emission lines as a gas laser medium.

Alexandrite laser crystal was developed by Walling and his co-workers [2,3] in early 1980s. It was used in some experiments [4–6], but it did not become as popular as the YAG crystal, mainly because of the technical difficulties in crystal growth, which should be overcome if there is sufficient demand for Alexandrite rods. In our view, the Alexandrite laser is an obvious candidate for a solid state laser to produce UV and DUV light for optical lithography and for other semiconductor industrial applications. The Alexandrite laser is tunable from 700 to 820 nm and it can generate powerful coherent light at 365 nm (by second harmonic from 730 nm), 248 nm (by third harmonic from 744 nm) and 193 nm (by fourth harmonic from 772 nm). The solid state Alexandrite laser produces much better coherent light than an excimer laser. A compact DUV 248 nm solid state laser from a Q-switched Alexandrite laser has been demonstrated [7]. Indeed, its optical and physical characteristics are comparable to those of the YAG crystal, as is illustrated in Table 1 [8]. In particular, the spontaneous lifetime is long enough to permit flash-lamp pumping.

In this paper, we report the achievement of a long pulse with low peak power at 365 nm, produced by the frequency-doubled output of an Alexandrite laser. This is ideal for some applications, for example in the semiconductor industry where minimal damage of the substrate is required. The capability of optical lithography is now such that

the limit in microelectronic fabrication is below 300 nm. It is necessary for metrology to also be extended to the minimum feature size, which can be produced by lithography. For measurements at this level of resolution a laser with a very long coherence length is highly desirable. Recently there has also been great interest in sub-micron three dimensions (3D) surface metrology for device characterisation and checking defects. A high energy, low peak power UV laser source, similar to that described in this work, was used in UV microscopy to measure 3D features as small as 300 nm [9].

A 365 nm UV laser can also be used in other applications, such as removing surface defects in a single shot. The high energy laser at 365 nm also provides a powerful tool to photo-sensitise polymer material, where both high resolution and high energy is achieved.

2. Design of the resonator and experiments with high energy long pulse at 730 nm

In contrast to previous work, we examine the characteristics of the Alexandrite laser on the short wavelength side of its gain profile, primarily at 730 nm.

A schematic diagram of the laser configuration is shown in Fig. 1. The laser head consists of two 100 mm arc-length flash-lamps of 350 Torr pressure, a double ellipse glass condenser coated with silver to ensure high pump efficiency and an Alexandrite laser rod, which was produced by Allied Corp. with 0.2% Cr^{3+} atomic concentration, is 7 mm in diameter and 127 mm in length and both ends were antireflection coated for 720–730 nm.

Table 1
Comparison of main characteristics of Alexandrite and Nd:YAG

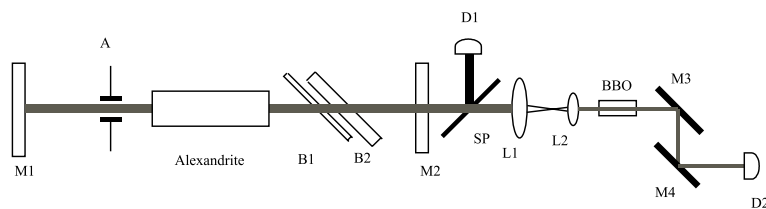| Properties	Alexandrite $BeAl_2O_4$:Cr^{3+}	Nd:YAG Nd:$Y_3Al_5O_{12}$
Laser wavelength (nm)	700–820	1064, 1061
Spontaneous lifetime (μs)	260 ($T = 298$ K)	230
Melting point (°C)	1870	1970
Thermal expansion	6×10^{-6} K^{-1}	7.8×10^{-6} K^{-1}
Thermal conductivity (W cm^{-1} K^{-1})	0.23	0.14
Doping density (at.%)	0.05–0.4	0.03–1

Fig. 1. Schematic diagram of the laser configuration. M1, M2: resonator mirrors, Alexandrite: laser rod, A: Aperture, D1, D2: energy metres, B1, B2: birefringent plate, SP: beam splitter, L1, L2: step-down lenses, BBO: frequency doubling crystal, M3, M4: high reflection mirrors at 365 nm.
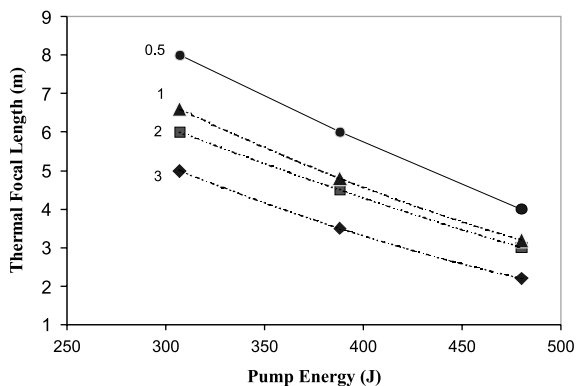

Fig. 2. Thermal focal length of Alexandrite as a function of pump energy for repetition rate: (◆) 3 Hz, (■) 2 Hz, (▲) 1 Hz and (●) 0.5 Hz.

Fig. 3. Energy level diagram for chromium ions in Alexandrite.

Before designing a laser resonator the thermal lens effect of the rod was studied. For pump repetition rates of 3, 2, 1 and 0.5 Hz, the effective thermal lens focal lengths were measured and these are plotted in Fig. 2. Subsequently, a laser resonator of 90 cm in length was built. It is terminated by two flat mirrors, one of high reflectivity at 720–730 nm and the other allowing 50% transmission for the same wavelength band. The laser resonator always satisfies the criterion of a stable cavity within the range of the thermal lens. An home made variable aperture with maximum 4 mm and minimum 1 mm diameter was placed in the cavity where the distance between the centre of the laser rod and the aperture is 100 mm, to confine the laser beam to be a TEM_{00} mode. Since the diameter of TEM_{00} in the place where aperture is located in between 1.4 and 1.27 mm under the condition of 1 Hz repetition and 300–480 J energy pump level. An 1-mm-thick glass tube surrounds the laser rod to prevent rod solarisation by UV
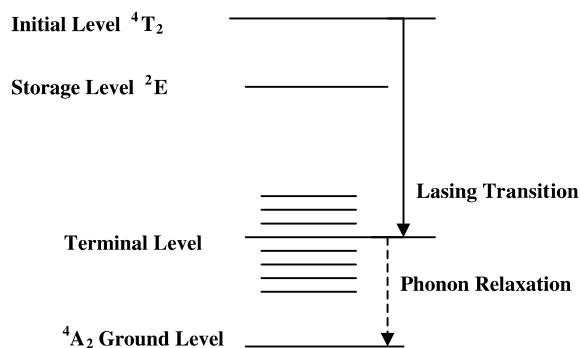
light from the pump lamps. The glass tube also serves to guide the cooling water in the head. To tune the laser wavelength of the Alexandrite medium, two birefringent plates are used, one of them is 0.5 mm thick, the other 2 mm.

Performance of an Alexandrite crystal is highly temperature dependent. At low temperature (about 77 K), the crystal acts as a three-level laser and emits the 680 nm R-line. The transition operates between the metastable level ^2E and the ground level $^4A_2$ (Fig. 3). At a higher temperature, the three-level mode gives way to a four-level mode and the transition operates between initial level $^4T_2$ and the vibronic terminal level. At still higher temperatures, more vibronic continua in $^4T_2$ level will be gradually gathered from the metastable level ^2E due to the action of Boltzmann distribution and the stimulated cross-section will increase. But the higher temperature also causes the population in the vibronic terminal level to increase, particularly for the terminal level which lies closest to the ground and which corresponds to the shortest wavelength emission. The laser transition often operates between those levels, where
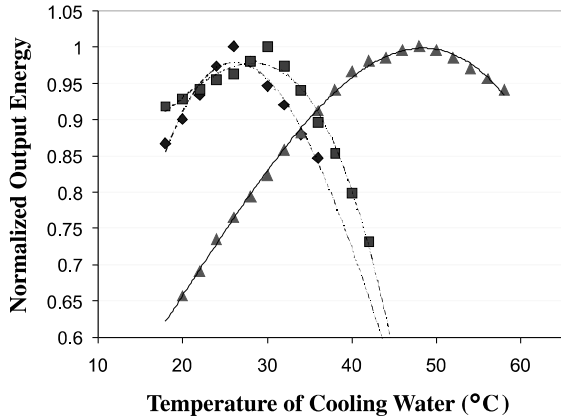
Fig. 4. Output energy (normalised to peak energy) at: (◆) 720 nm, (■) 725 nm, (▲) 730 nm from Alexandrite laser versus the temperature of cooling water for a fixed pump energy of 433 J (pulse repetition frequency:1 Hz).

the initial level populates much more and the terminal level populates the least. Therefore when the temperature rises, two conflicting effects occur [10]. A trend of temperature dependence is quite clear, but it would be difficult to accurately predict the optimum operation temperature for a given wavelength. Thus we determine the optimum temperature experimentally.

The curve of the normalised output at 1 Hz pulse repetition frequency at 730 nm versus the coolant temperature is shown in Fig. 4. As discussed above, the curve shows that if the input electric energy is fixed, the laser output at 730 nm increases as the temperature of the coolant rises to about 46 °C where the peak energy is 2.24 J for a fixed pump energy of 433 J. The gain of the Alexandrite laser decreases beyond this turning point because the population increase in the vibronic terminal level exceeds that of the vibronic continua in the $^4T_2$ level. Thus the optimum coolant temperature for highest output at 730 nm should be close to that at the turning point. For the same pump energy of 433 J the normalised output energy at 725 and 720 nm as a function of the cooling water temperature is also shown in Fig. 4. The curves show that the optimum cooling water temperature is lower for these wavelengths. The optimum temperatures for 720 and 725 nm, producing peak energies of 206 and 899 mJ/pulse respectively, are 26 and 30 °C.
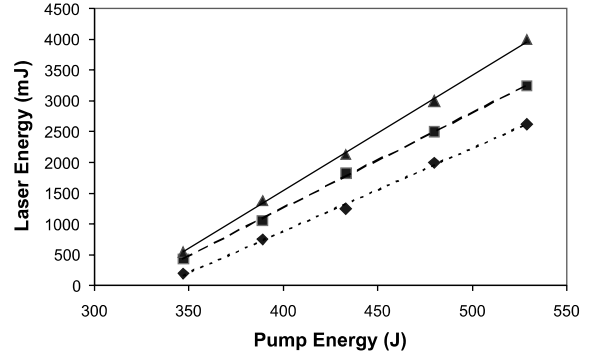

Fig. 5. The output power of Alexandrite laser at 730 nm versus the input electric power at different cooling water temperature: (◆) 20 °C, (■) 33 °C, (▲) 46 °C (pulse repetition frequency:1 Hz).
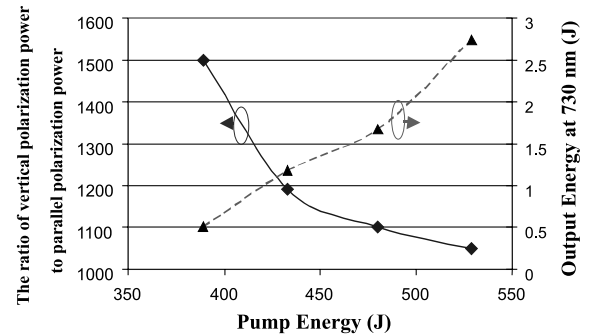

Fig. 6. Depolarisation of Alexandrite laser at 730 nm versus different input electric energy (■), output energy (▲).

Fig. 5 shows the output power of Alexandrite laser at 730 nm versus the input electric power at different cooling water temperature at 1 Hz pulse repetition frequency. The curves show that the slope efficiency is maximum when the laser operates at optimum cooling water temperature. The depolarisation of the Alexandrite laser at 730 nm has also been measured and it is plotted in Fig. 6. The plot shows that the depolarisation of the Alexandrite medium is not severe with the rise of input pump energy, the polarisation ratio never dropping below 1000:1.

3. Second harmonic generation

Beta barium borate (BBO) and Lithium triborate (LBO) are two well-known crystals for fre-

quency doubling, especially for generating UV light. Compare with BBO, LBO has a higher damage threshold, allowing use of higher intensities, and a much reduced walk-off angle, allowing use of a longer crystal, but BBO has a higher effective nonlinear coefficient (1.7 times that of the LBO). In our laser, we chose BBO as the frequency doubling crystal, since the intensity is not very high, and the crystal length can be shorter, so the expense of the laser can be reduced. To enhance the second harmonic efficiency, type I critical phase matching is used. The calculated effective coefficient is 3.47 times that of KDP and the phase matching angles θ, ϕ, walk-off angle and acceptance angle $\Delta\theta$ are 32.13°, 0°, 4.16° and 0.3 mrad cm respectively. The dimension for the BBO crystal used in this work are 5 mm × 5 mm × 10 mm. The two end faces were antireflection coated for 730 and 365 nm respectively by the manufacturer, Shandong University, P.R. China.

High frequency doubling efficiency requires high fundamental peak power. For our long pulse laser (220 μs), the BBO crystal can be either inside or outside the resonator. If the SHG medium is put into the resonator, the peak power passing through the BBO crystal can be enhanced, but the generated 365 nm light penetrates the Alexandrite rod and may solarise the medium. To prevent this it is necessary to insert a filter into the resonator, which may result in increased intracavity losses and in a decrease in output. Thus we chose to place the BBO crystal outside the cavity. In order to achieve high peak power from a long pulse laser, one can either use a second cavity or made the beam diameter become small. The former need an electronic system to lock the cavity, the laser expense will increase, thus the latter was chosen. If a short focusing lens is used, the beam diameter can be much small, but the divergence angle of the laser beam will increase quickly. This will depress the efficiency of nonlinear conversion because of the small acceptance angle and large walk-off angle of a BBO crystal. In order for the beam divergence angle not to become too great, a telescope system that consists of two high quality lenses with surfaces antireflection coated at 720–730 nm and focal lengths of 150 and 35 mm, were used. The spot size in the BBO crystal is 1 mm. This beam size is larger
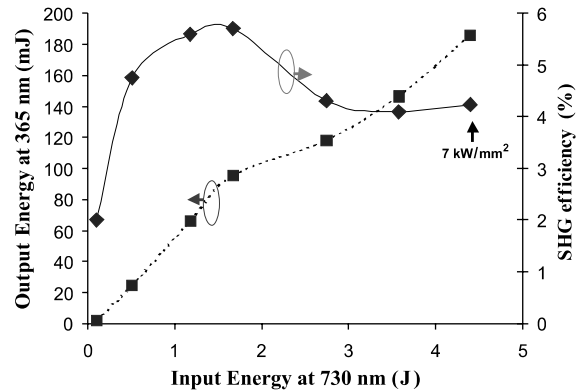

Fig. 7. Output of 365 nm versus energy of 730 nm (■) and second harmonic generation efficiency (◆) at 365 nm from 730 nm.

than the walk-off distance of 0.73 mm at the output face of the BBO crystal and the beam divergence angle in BBO crystal is about 4 mrad. The energy of 365 nm UV light and the frequency-doubling efficiency versus the input energy at 730 nm, are depicted in Fig. 7. The maximum SHG output energy at 365 nm was 186 mJ/pulse and was generated from a 4.4 J, 730 nm pulse with low peak power of 7 kW/mm^2. The curves also show that the SHG energy increases monotonically with increase in input energy, but the efficiency peaks at 5.7%, before dropping to about 4.2%. The explanation is that the fundamental laser peak power increases with the input pump energy increase until the frequency-doubling efficiency reaches 5.7%. When the input energy increases further, the thermal focal length of the laser rod, which varies from 3 to 8 m under input energies used in this work, becomes short enough to permit the TEM_{01} mode to resonate in the cavity. The SHG efficiency drops as the result of the fundamental beam divergence angle increasing.

4. Conclusion

An high energy long pulse at 365 nm laser has been described. It is energetic enough to meet general applications in optical lithography and polymer material processing. The SHG efficiency of this experiment is limited by the low acceptance angle and the large beam walk-off angle in BBO

crystal. The laser can be improved by using two properly oriented crystals to compensate for the walk-off and to reduce the divergence angle of the fundamental laser beam in the SHG. A much stronger UV laser should be realised. Moreover, a 248 and 193 nm laser from Alexandrite crystal can be generated by the third harmonic from 744 nm and fourth from 772 nm.

Acknowledgements

References

[1] M. Kuwahara, T. Nakano, J. Tominaga, M.B. Lee, N. Atoda, High-speed optical near-field photolithography by super resolution near-field structure, Jpn. J. Appl. Phys. 38 (1999) L1079–L1081.

[2] J.C. Walling, O.G. Peterson, H.P. Jenssen, R.C. Morris, E.W. O'dell, Tunable Alexandrite lasers, IEEE J. Quant. Electron. QE-16 (12) (1980) 1302–1315.

[3] J.C. Walling, D.F. Heller, H. Samelson, D.J. Harter, J.A. Pete, R.C. Morris, Tunable Alexandrite lasers, IEEE J. Quant. Electron. QE-21 (1985) 1568–1581.

[4] S. Imai, H. Ito, Long-pulse ultraviolet-laser source based on tunable Alexandrite laser, IEEE J. Quant. Electron. QE-34 (1988) 573–576.

[5] V. Meyer, S.N. Bagayev, P.E.G. Baird, P. Bakule, M.G. Boshier, A. Breitrück, et al., Measurement of the 1s–2s energy interval in muonium, Phys. Rev. Lett. 84 (2000) 1136–1139.

[6] P. Bakul, P.E.G. Baird, M.G. Boshier, S.L. Cornish, D.F. Heller, K. Jungmann, A chirp-compensated, injection-seeded Alexandrite laser, Appl. Phys. B Lasers Opt. 71 (2000) 11–17.

[7] J.W. Kuper, T.C. Chin, P.A. Papanestor, High average power, narrow band 248 nm Alexandrite laser system, SPIE 2115 (1994) 88.

[8] W. Koechner, Solid-State Laser Engineering, Fifth Revised and Updated Edition, Springer, p. 73.

[9] P.C. Montgomery, D. Montaner, Deep submicron 3D surface metrology for 300 mm wafer characterisation using UV coherence microscopy, Microelectron. Eng. 45 (1999) 291–297.

[10] W. Koechner, Solid-State Laser Engineering, Fifth Revised and Updated Edition, Springer, p. 75.